
# Mononuclear dioxomolybdenum(VI) thiosemicarbazonato complexes: Synthesis, characterization, structural illustration, *in vitro* DNA binding, cleavage, and antitumor properties

Mouayed A. Hussein, Teoh S. Guan, Rosenani A. Haque, Mohamed B. Khadeer Ahamed, Amin M.S. Abdul Majid

PII: S1386-1425(14)01517-0
DOI: http://dx.doi.org/10.1016/j.saa.2014.10.021
Reference: SAA 12835

To appear in: *Spectrochimica Acta Part A: Molecular and Biomolecular Spectroscopy*

Received Date: 6 April 2014
Revised Date: 13 August 2014
Accepted Date: 9 October 2014

Please cite this article as: M.A. Hussein, T.S. Guan, R.A. Haque, M.B. Khadeer Ahamed, A.M.S. Abdul Majid, Mononuclear dioxomolybdenum(VI) thiosemicarbazonato complexes: Synthesis, characterization, structural illustration, *in vitro* DNA binding, cleavage, and antitumor properties, *Spectrochimica Acta Part A: Molecular and Biomolecular Spectroscopy* (2014), doi: http://dx.doi.org/10.1016/j.saa.2014.10.021

# Mononuclear dioxomolybdenum(VI) thiosemicarbazonato complexes: Synthesis, characterization, structural illustration, *in vitro* DNA binding, cleavage, and antitumor properties

**Mouayed A. Hussein [a], Teoh S. Guan[a*], Rosenani A. Haque[a], Mohamed B. Khadeer Ahamed[b], Amin M.S. Abdul Majid[b]**

[a] School of Chemical Science, Universiti Sains Malaysia, 11800 – Minden, Pulau Pinang, Malaysia

[b] EMAN Research and Testing Laboratory, School of Pharmaceutical Sciences, Universiti Sains Malaysia, 11800 – Minden, Pulau Pinang, Malaysia

*Corresponding author: Dr. Teoh Siang Guan, PhD,
Professor
School of Chemical Sciences
Universiti Sains Malaysia
Penang-11800, Malaysia
E-mail: sgteoh@usm.my
H/P : (604) – 6577888
Fax : (604) - 6574854

**Abstract**

Four dioxomolybdenum(VI) complexes were synthesized by reacting $[MoO_2(acac)_2]$ with *N*-ethyl-2-(5-bromo-2-hydroxybenzylidene) hydrazinecarbothioamide (**1**), *N*-ethyl-2-(5-

allyl-3-methoxy-2-hydroxybenzylidene) hydrazinecarbothioamide (**2**), N-methyl-2-(3-*tert*-butyl-2-hydroxybenzylidene) hydrazinecarbothioamide (**3**), and *N*-ethyl-2-(3-methyl-2-hydroxybenzylidene) hydrazinecarbothioamide (**4**). The molecular structures of **1**, **2**, and all the synthesized complexes were determined using single crystal X-ray crystallography. The binding properties of the ligand and complexes with calf thymus DNA (CT-DNA) were investigated via UV, fluorescence titrations, and viscosity measurement. Gel electrophoresis revealed that all the complexes cleave pBR 322 plasmid DNA. The cytotoxicity of the complexes were studied against the HCT 116 human colorectal cell line. All the complexes exhibited more pronounced activity than the standard reference drug 5-fluorouracil ($IC_{50}$ 7.3 μM). These studies show that dioxomolybdenum(VI) complexes could be potentially useful in chemotherapy.

*Key words*: Thiosemicarbazone, Molybdenum(VI) complexes, X-ray crystal structure, DNA binding, DNA cleavage, Antiproliferative activity.

## 1. Introduction

The biological and pharmacologic studies on thiosemicarbazones have received increasing interest because of their antitumor, antifungal, and antiviral activities [1,2] and recently, their effectiveness against *Mycobacterium tuberculosis* [3,4]. Thiosemicarbazones belong to big group of thiourea derivatives whose biological actions depend on a parent moiety of aldehyde or ketone [5,6]. The tridentate ONS ligand system of thiosemicarbazide exhibits anticancer activity because of a structural modification that impedes the chelating capability of thiosemicarbazones, which removes or minimizes its medicinal action [7]. However, the presence of metal ions usually increases the activity, which is comparable to that of the corresponding ligands [8].

Metal chelation is useful in producing new chemical features of metal complexes to make them suitable for pharmacologic applications. Many useful drugs have metal-binding sites that may change their physiologic profile when in their free form. Some drugs form chelates with specific metal ions that increases their activity [9].

Molybdenum has been widely investigated in recent years because of its intrinsic importance for almost all biological systems: it is required by enzymes that catalyze the metabolism of sulfur, carbon, and nitrogen. It participates in a broad range of metalloenzymes in algae, bacteria, fungi, plants, and animals, wherein molybdenum forms part of the active sites of these enzymes [10,11].Various molybdenum complexes have been prepared and subjected for multiple pharmaceutical purposes wherein their anticancer activity received special interest [12,13].

Dioxomolybdenum(VI) complexes ONS donor ligands have received considerable interest as a mimicry system for the active sites of molybdoenzymes, such as xanthine oxidase and DMSO reductase, which have oxo-molybdenum cores with a molybdenum atom that coordinates with two or more sulfur donor ligands [14-16]. This study describes the synthesis, characterization, DNA interaction/cleavage, and antitumor activity of a series of *cis*-dioxomolybdenum(VI) complexes with some of 4-methyl (or ethyl) thiosemicarbazones shown in Scheme 1.

## 2. Experimental

### 2.1. Materials and instrumentation

Melting points were measured using a Stuart Scientific SMP1 melting point apparatus. The infrared (IR) spectra were recorded on a Perkin Elmer system 2000 spectrophotometer using the KBr disc method. The $^{1}H$ and $^{13}C$ NMR spectra were recorded on a Bruker 500 $MH_z$ and 400 $MH_z$, respectively, using tetramethylsilane as the internal standard and DMSO-$d_6$ as the

solvent. Elemental analysis was carried out using a Perkin Elmer 2400 series-11 CHN analyzer. The electronic and fluorescent spectra were recorded on a Perkin Elmer Lambda-35 spectrophotometer and a Jasco FP-750 spectrophotometer, respectively. X-ray crystallographic data were recorded on a Bruker SMART CCD diffractometer using graphite monochromated Mo Kα radiation ($\lambda = 0.71073\ A^0$) at 100 K. The data collected were reduced using SAINT program. The structure of all compounds was solved using the SHELXL-97 software package, and the molecular graphics were created using SHELXTL [17]. All non-hydrogen atoms were anisotropically refined. All of the chemicals, including thiosemicarbazide, aldehydes, and the solvents were purchased from Sigma-Aldrich.

### 2.2. DNA binding assay

The binding of complexes with CT DNA were investigated in 6.3 mM Tris-HCl/50 mM NaCl buffer (pH = 7). The DNA stock solution was prepared by dissolving a suitable amount of DNA in 6.3 mM Tris-HCl/50 mM NaCl buffer (pH = 7) at room temperature and stored in refrigerator for 2 days . A solution of CT DNA in the buffer provided a UV absorbance ratio at 260 nm and 280 nm of ca. 1.9:1, which indicates that the DNA was sufficiently free of protein. The DNA concentration was estimated by the UV absorbance at 260 nm using the known molar absorption coefficient of 6600 $M^{-1}\ cm^{-1}$ [18]. The UV-Vis spectra were scanned at wavelengths ranging from 230 nm to 600 nm using the Tris/HCl buffer solution as the reference.

A fluorescence emission assay was carried out using the aforementioned method. The fluorescence spectra were scanned at wavelengths ranging from 200 nm to 800 nm using the Tris/HCl buffer solution as the reference.

Viscosity was measured using a Cannon Manning Semi-Micro viscometer immersed in a thermostatic water bath at 37 °C. Flow times were measured manually with a digital

stopwatch. The viscosity values were calculated from the observed flow time of DNA-containing solutions ($t$) corrected for that of solvent mixture used ($t_0$), $\eta = t - t_0$. The viscosity data are presented as $(\eta/\eta_0)^{1/3}$ versus the ratio of the concentration (r) of the ligand or complex-DNA solutions, where $\eta$ and $\eta_0$ are the viscosity of the complex in presence of DNA and the viscosity of DNA alone, respectively [19].

### 2.3. DNA cleavage study

The activity of the ligands and the complexes to cleave pBR322 plasmid DNA was determined using agarose gel electrophoresis in Tris/EDTA buffer solution. The samples were incubated at 37 °C for 2 h, treated with loading dye, and electrophoresed for 1 h at 50 V on 1% agarose gel. The gel was then stained with ethidium bromide before being photographed under UV light.

### 2.4. Antiproliferation assay

#### 2.4.1. Preparation of cell culture

Human colorectal cancer cells (HCT 116) were grown under optimal incubator conditions. The cells that reached 70%–80% confluence were chosen for cell plating purposes. The old medium was replaced by aspiration. After washing the cells 2–3 times with sterile phosphate buffered saline (PBS) (pH 7.4), the intact layer of attached cells was trypsinized. The cells were incubated at 37 °C in 5% $CO_2$ for 3 min to 5 min. Then, the flasks containing the cells were gently tapped to aid cells segregation and observed under an inverted microscope (to confirm the completion of cell segregation). Trypsin activity was inhibited by adding 5 mL of fresh complete media supplied with 10% fetal bovine serum (FBS). The cells were counted and diluted to a final concentration of $2.5 \times 10^5$ cells/mL, and

inoculated into wells (100 µL/well). Finally, the plates containing the cells were incubated at 37 °C with an internal atmosphere of 5% $CO_2$.

2.4.2. MTT assay

Cytotoxicity of the compounds was evaluated using an MTT assay [20] against HCT 116 cells. The HCT 116 cells ($1.5 \times 10^5$ cells/mL, 100 µL/well) were seeded into a 96-well microtiter plate. Then, the plate was incubated overnight in a $CO_2$ incubator for to allow the cell for attachment. Then, 100 µL of the test substance was added into each well containing the cells. The test substance was diluted with media to the desired concentrations from the stock. The plates were incubated at 37 °C with an internal atmosphere of 5% $CO_2$ for 72 h. After this treatment period, 20 µL of MTT reagent was added into each well and incubated again for 4 h. After this incubation period, 50 µL of MTT lysis solution (DMSO) was added into the wells. The plates were further incubated for 5 min in a $CO_2$ incubator. Finally, the plates were read at 570 nm and 620 nm wavelengths using a standard ELISA microplate reader. The data were recorded and analyzed to assess the effects of the test substance on cell viability. The percentage of growth inhibition was calculated from the optical density (OD) that was determined from the MTT assay, i.e., the hundredth multiple of the subtracted OD value of the control and the surviving cells over the OD of the control cells.

2.5. Synthesis of ligands

2.5.1. Synthesis of *N*-ethyl-2-(5-bromo-2-hydroxybenzylidene) hydrazinecarbothioamide (**1**)

A solution of 5-bromo-2-hydroxybenzaldehyde (0.84 g, 4.19 mmol) in ethanol (20 mL) was added to 4-ethyl-3-thiosemicarbazide (0.5 g, 4.19 mmol) in ethanol (20 mL). The resulting yellow solution was refluxed with stirring for 2 h and then filtered .The filtrate was left to stand at room temperature for two days to obtain a block yellow crystals. M.p: 201 °C to

203 °C, (0.94 g, 75%). Anal. Calc. for $C_{10}H_{12}BrN_3OS$: C, 39.70%; H, 3.97%; N, 13.89%, found: C, 39.73%; H, 3.95%; N, 13.88%; IR(KBr) ($\nu_{max}$/cm$^{-1}$): 3302 (m, NH), 3147 (m, OH), 1600–1613 (m, C=N-N-C), 1550 (m, $C_{aro}O$), 1268 (m, C=S); $^1$H NMR (DMSO-$d_6$, ppm): 1.11 (t, 2H, J=7 Hz, $CH_3$), 3.56 (qn, 4H, J=7 Hz, $CH_2$), 6.80 (d, 1H, J=8.5 Hz, H-3), 7.31 (d, 1H, J=8.5 Hz, H-4), 8.08 (s, 1H, H-6), 8.27 (s, 1H, CH=N), 8.57 (t, 2H, br, CS-NH), 11.30 (s, 1H, N-NH); $^{13}$C NMR (DMSO-$d_6$,ppm): 14.48 ($CH_3$), 30.55 ($CH_2$), 111.06-137.59 (C-aromatic), 155.40 (C=N), 176.37 (C=S).

2.5.2. Synthesis of *N*-ethyl-2-(5-allyl-3-methoxy-2- hydroxybenzylidene) hydrazinecarbothioamide (**2**)

A solution of 5-allyl-3-methoxy-2-hydroxybenzaldehyde (0.80 g, 4.19 mmol) in ethanol (20 mL) was added to a solution of 4-ethyl-3-thiosemicarbazide (0.5 g, 4.19 mmol) in ethanol (20 mL). The resulting colorless solution was refluxed with stirring for 2 h. A white fluffy product was formed when the solution was cooled to room temperature, filtered, washed with ethanol, and air-dried. M.p: 193 °C to 195 °C, (0.98 g, 80%). Anal. Calc. for $C_{14}H_{19}N_3O_2S$: C, 57.25%; H, 6.47%; N, 14.31%, found: C, 57.24%; H, 6.49%; N, 14.32%; IR(KBr) ($\nu_{max}$/cm$^{-1}$): 3312 (s, NH), 1585 (m, C=N), 1544 (s, $C_{aro}O$), 1277 (m, C=S); $^1$H NMR (DMSO-$d_6$, ppm): 1.15 (t, 2H, J=7 Hz, $CH_3$), 3.30 (d, 1H, J=6.5 Hz, $CH_2$-Ph), 3.60 (qn, 4H, J=7 Hz, $CH_2$), 3.79 (s, 3H, O-$CH_3$), 5.02 (dd, J=10 Hz, J=17.5 Hz, $CH_2$=), 6.02 (m, 4H, =CH), 6.78(s, 1H, H-4), 7.34 (s, 1H, H-6 H), 8.37 (t, 2H, br, CS-NH), 8.39 (s, 1H, CH=N), 9.09 (s, 1H, OH), 11.40 (s, 1H, N-NH); $^{13}$C NMR (DMSO-$d_6$,ppm): 14.61 ($CH_3$), 38.24 ($CH_2$), 55.85 (O-$CH_3$), 113.16 ($CH_2$ -Ph), 115.46 ($CH_2$=), 117.49 (=CH), 120.83-147.88 (C-aromatic), 155.85 (C=N), 177.52 (C=S).

2.5.3. Synthesis of N-methyl-2-(3-*tert*-butyl-2- hydroxybenzylidene) hydrazinecarbothioamide (**3**)

A solution of 3-*tert*-butyl-2-hydroxybenzaldehyde (0.84 g, 4.75 mmol) in ethanol (20 mL) was added to a solution of 4-methyl-3-thiosemicarbazide (0.5 g, 4.75 mmol) in ethanol (20 mL). The resulting colorless solution was refluxed with stirring for 2 h and then filtered. The filtrate was left to stand at room temperature for 2 days, and formed a white product. M.p: 177 °C to 179 °C, (0.95 g, 76%). Anal. Calc. for $C_{13}H_{19}N_3OS$: C, 58.78%; H, 7.15%; N, 15.82%, found: C, 58.77%; H, 7.13%; N, 15.81%; IR(KBr) ($\nu_{max}$/cm$^{-1}$): 3428 (m, NH), 3150 (m, OH), 1599 (s, C=N), 1553 (s, $C_{aro}O$), 1266 (s, C=S); $^1$H NMR (DMSO-$d_6$, ppm): 1.40 [s, 9H, $(CH_3)_3$], 3.02 (d, 1H, J=4.5 Hz, $CH_3$), 6.87(t, 2H, J=7.5 Hz, H-5), 7.24(d, 1H, J=7 Hz, H-4), 7.28 (d, 1H, J=8 Hz, H-6), 8.29 (s, 1H, CH=N), 8.45 (q, 3H, br, CS-NH), 10.02 (s, 1H, OH), 11.28 (s, 1H, N-NH); $^{13}$C NMR (DMSO-$d_6$,ppm): 29.35 [$(CH_3)_3$], 31.16 [ $\underline{C}(CH_3)_3$], 34.45 ($CH_3$), 118.65-146.64 (C-aromatic), 155.19 (C=N), 177.36 (C=S).

2.5.4. Synthesis of *N*-ethyl-2-(3-methyl-2-hydroxybenzylidene) hydrazinecarbothioamide (**4**)

A solution of 5-methyl-2-hydroxybenzaldehyde (0.57 g, 4.19 mmol) in ethanol (20 mL) was added to a solution of 4-ethyl-3-thiosemicarbazide (0.5 g, 4.19 mmol) in ethanol (20 mL). The resulting colorless solution was refluxed with stirring for 2 h and then filtered. The filtrate was left to stand at room temperature for 2 days to obtain a block colorless crystals. M.p: 187 °C to 189 °C, (0.76 g, 76%). Anal. Calc. for $C_{11}H_{15}N_3OS$: C, 55.61%; H, 6.32%; N, 17.69%, found: C, 55.63%; H, 6.31%; N, 17.68%; IR(KBr) ($\nu_{max}$/cm$^{-1}$): 3412 (m, NH), 3169 (s, OH), 1605 (s, C=N), 1268 (m, C=S); $^1$H NMR (DMSO-$d_6$, ppm): 1.15 (t, 2H, J=7 Hz, $CH_3$), 2.20 (s, 3H, $H_3C$-Ph), 3.59 (qn, 4H, J=6.5 Hz, $CH_2$), 6.82(t, 2H, J=7.5 Hz, H-5), 7.18(d, 1H, J=7.5 Hz, H-4), 7.41 (d, 1H, J=7.5 Hz, H-6), 8.34 (s, 1H, CH=N), 8.49 (t, 2H, br, CS-NH), 9.69 (s, 1H, OH), 11.30 (s, 1H, N-NH); $^{13}$C NMR (DMSO-$d_6$,ppm): 14.48 ($CH_3$), 15.86 ($CH_3$-Ph), 30.59 ($CH_2$), 119.02-143.91 (C-aromatic), 154.23 (C=N), 176.47 (C=S).

2.6. Synthesis of complexes

2.6.1. Synthesis of *N*-ethyl-2-(5-bromo-2-hydroxybenzylidene) hydrazinecarbothioamide dioxomolybdenum (VI) (**1a**)

A solution of $MoO_2(acac)_2$ (0.1 g, 0.306 mmol) in methanol (25 mL) was added to a solution of **1** (0.092 g, 0.306 mmol) in methanol (25 mL). The resulting red solution was refluxed for 2 h and then filtered. The filtrate was left to stand at room temperature for 5 days to obtain a block orange crystals. M.p: 240 °C–242 °C, (0.13 g, 80%). Anal. Calc. for $C_{12}H_{17}BrMoN_3O_5S$: C, 29.31%; H, 3.46%; N, 8.55%; Mo, 19.53%, found: C, 29.34%; H, 3.45%; N, 8.57%; Mo, 19.48%; IR(KBr) ($\nu_{max}/cm^{-1}$): 3295 (m, NH), 1590 (s, C=N), 1548 (m, $C_{aro}O$), 1266 (s, C-S), 942,902 (s, Mo=O); $^1H$ NMR (DMSO-$d_6$, ppm): 1.12 (t, 2H, J=7 Hz, $CH_3$), 3.18 (s, 3H, alcoholic-$CH_3$), 3.28 (qn, 4H, J=6.5 Hz, $CH_2$), 6.83(d, 1H, J=9 Hz, H-3), 7.51(dd, 2H, J=9 Hz, J=2.5 Hz, H-4), 7.84 (d, 1H, J=2.5 Hz, H-6), 7.64 (t, 2H, br, CS-NH), 8.54 (s, 1H, CH=N); $^{13}C$ NMR (DMSO-$d_6$,ppm): 14.48 ($CH_3$), 30.55 ($CH_2$), 47.87 (alcoholic-$CH_3$), 118.15-137.00 (C-aromatic), 149.86 (C=N), 157.74 (C-S).

2.6.2. Synthesis of *N*-ethyl-2-(5-allyl-3-methoxy-2-hydroxybenzylidene) hydrazinecarbothioamide dioxomolybdenum (VI) (**2a**)

A solution of $MoO_2(acac)_2$ (0.1 g, 0.306 mmol) in ethanol (25 mL) was added to a solution of **2** (0.09 g, 0.306 mmol) in ethanol (25 mL). The resulting red solution was refluxed for 2 h and then filtered. The filtrate was left to stand at room temperature for 1 week to obtain a block red crystals. M.p: 185 °C–187 °C, (0.12 g, 82%). Anal. Calc. for $C_{14}H_{19}MoN_3O_5S$: C, 38.41%; H, 4.34%; N, 9.60%; Mo, 21.94%, found: C, 38.43%; H, 4.31%; N, 9.63%; Mo,

21.83%; IR(KBr) ($\nu_{max}$/cm$^{-1}$): 3309 (s, NH), 3447 (s, OH), 1589 (m, C=N), 1566 (s, $C_{aro}O$), 1270 (s, C-S), 936,902 (s, Mo=O); $^1$H NMR (DMSO-$d_6$, ppm): 1.12 (t, 2H, J=7 Hz, $CH_3$), 3..27 (qn, 4H, J=7 Hz, $CH_2$), 3.32 (d, 1H, J=6.5 Hz, $CH_2$-Ph), 3.79 (s, 3H, O-$CH_3$), 5.06 (dd, 1H, J=9.5 Hz, J=17 Hz, $CH_2$=), 5.99 (m, 4H, =CH), 6.78(s, 1H, H-4), 7.34 (s, 1H, H-6), 7.43 (t, 2H, br, CS-NH), 8.48 (s, 1H, CH=N); $^{13}$C NMR (DMSO-$d_6$,ppm): 14.61 ($CH_3$), 38.24 ($CH_2$), 55.81 (O-$CH_3$), 115.49 ($CH_2$ -Ph), 115.90 ($H_2C$=), 117.44 (=CH), 121.01-147.13 (C-aromatic), 148.01 (C=N), 151.18 (C-S).

2.6.3. Synthesis of *N*-methyl-2-(3-*tert*-butyl-2-hydroxybenzylidene) hydrazinecarbothioamide dioxomolybdenum (VI) (**3a**)

A solution of $MoO_2(acac)_2$ (0.1 g, 0.306 mmol) in methanol (25 mL) was added to a solution of **3** (0.081 g, 0.306 mmol) in methanol (25 mL). The resulting red solution was refluxed for 2 h and then filtered. The filtrate was left to stand at room temperature for 4 days to obtain a block brown crystals. M.p: 202 ° to 204 °C, (0.14 g, 92%). Anal. Calc. for $C_{14}H_{21}MoN_3O_4S$: C, 39.68%; H, 4.96%; N, 9.92; Mo, 22.66%, found: C, 39.66%; H, 4.95%; N, 9.91%; Mo, 22.48% IR(KBr) ($\nu_{max}$/cm$^{-1}$): 3366 (m, NH), 1585 (s, C=N), 1561 (s, $C_{aro}O$), 932,893 (s, Mo=O); $^1$H NMR (DMSO-$d_6$, ppm): 1.35 [s, 9H, $(CH_3)_3$], 2.82 (d, 1H, J=4Hz, $CH_3$), 3.18 (s, 3H, alcoholic-$CH_3$), 6.92(t, 2H, J=7.5 Hz, H-5), 7.38(d, 1H, J=7 Hz, H-4), 7.48 (d, 2H, J=7.5 Hz, H-6), 7.43 (q, 3H, br, CS-NH), 8.55 (s, 1H, CH=N); $^{13}$C NMR (DMSO-$d_6$,ppm): 29.40 [$(CH_3)_3$], 30.78 [ $\underline{C}(CH_3)_3$], 34.55 ($CH_3$), 48.57 (alcoholic-$CH_3$), 120.37-146.55 (C-aromatic), 152.14 (C=N), 164.74 (C-S).

2.6.4. Synthesis of *N*-ethyl-2-(3-methyl-2-hydroxybenzylidene) hydrazinecarbothioamide dioxomolybdenum (VI) (**4a**)

A solution of $MoO_2(acac)_2$ (0.1 g, 0.306 mmol) in ethanol (25 mL) was added to a solution of **4** (0.072 g, 0.306 mmol) in ethanol (25 mL). The resulting red solution was refluxed for 2 h

and then filtered. The filtrate was left to stand at room temperature for 1 week to obtain plate orange crystals. M.p: 217 °C to 219 °C, (0.12 g, 79%). Anal. Calc. for $C_{11}H_{13}MoN_3O_4S$: C, 34.62%; H, 3.93%; N, 11.01%; Mo, 25.30%, found: C, 34.60%; H, 3.95%; N, 11.00%; Mo, 25.19%; IR(KBr) ($\nu_{max}/cm^{-1}$): 3295 (s, NH), 1595 (s, C=N), 1274 (m, C-S), 944,905 (s, Mo=O); $^1$H NMR (DMSO-$d_6$, ppm): 1.13 (t, 2H, J=7 Hz, $CH_3$), 2.15 (s, 3H, $H_3C$-Ph), 3.27 (qn, 4H, J=7 Hz, $CH_2$), 6.89(t, 2H, J=7 Hz, H-5), 7.32(d, 1H, J=6.5 Hz, H-4), 7.43 (d, 1H, J=7 Hz, H-6), 7.45 (t, 2H, br, CS-NH), 8.52 (s, 1H, CH=N); $^{13}$C NMR (DMSO-$d_6$,ppm): 14.42 ($CH_3$), 15.98 ($CH_3$-Ph), 30.65 ($CH_2$), 120.42-143.01 (C-aromatic), 151.66 (C=N), 156.99 (C-S).

## 3. Results and discussion

### 3.1. Synthetic aspects

New dioxomolybdenum (VI) complexes were synthesized by reacting $[MoO_2(acac)_2]$ with Schiff bases derived from 4-ethyl(methyl)thiosemicarbazone and 5-bromo-2-hydroxybenzaldehyde (**1**), 5-allyl-2-hydroxy-3-methoxybenzaldehyde (**2**), 3-*tert*-butyl-2-hydroxybenzaldehyde (**3**), and 2-hydroxy-3-methylbenzaldehyde (**4**). The ligands were prepared through the condensation of thiosemicarbazone with salicylaldehyde derivatives [21]. In all complexes, the ligands are coordinated as tridentate ligands via phenolic–oxygen, imine–nitrogen, and thiol–sulfur interactions. The sixth coordination site (**D**) required that the octahedral configuration of Mo is occupied by the solvent molecule. The X-ray crystal structure showed the distorted octahedral complexes of *cis*-dioxo-molybdenum(VI), where the D site was either $CH_3OH$ when it was used as solvent, as in **1a** and **3a** or $H_2O$ when ethanol (97%) was used as solvent, as in **2a** and **4a**. All the ligands and the complexes are air-stable and highly soluble in DMSO and DMF. Moreover, the ligand and their complexes are insoluble and highly stability in aqueous solutions. $^1$H NMR and UV spectra were recorded

after preparation, 7 day, 30 days, 3 months and 8 months, while kept at room temperature. All spectra confirmed the stability of the ligand and complexes in aqueous solutions.

The ligands **1–4** displayed FTIR, $^{1}$H NMR, and $^{13}$C NMR spectra and elemental analysis characteristics consistent with their assigned structures. In the FTIR, the bands ranging from 1585 $cm^{-1}$ to 1605 $cm^{-1}$ are attributed to the (C=N) group and the bands ranging from 1266 $cm^{-1}$ to 1277 $cm^{-1}$ are attributed to the (C=S) group [22]. In the $^{1}$H NMR, the triplet signal at 1.11 ppm is attributed to the protons of the ($-CH_3$) group of the complexes **1**, **2**, and **4**, whereas that for the complex **3** appeared at 3.02 ppm as a doublet signal. The quintet signal at 3.56 ppm or 3.60 ppm is attributed to the protons of the ($-CH_2$) group. The triplet signal at 8.57 ppm, 8.37 ppm and 8.49 ppm, and the quartet signal at 8.45 is attributed to the proton of the (CS-NH) group of the complexes **1**, **2**, **4**, and **3**, respectively. The signal of CS-NH group is attributed to the interaction of N-H with neighbor $CH_2$ protons of **1**, **2** and **4** or $CH_3$ protons of **3** which lead to produce a broad triplet or quartet signals, respectively. The broad signal peaks is attributed to the nuclear quadrupole interaction of $^{14}$N (I=1) which leads to lower the lifetime of H excited states. The aromatic proton signals are observed from 6.80 ppm to 8.08 ppm. In ligand **1**, the doublet signals of aromatic protons at 6.80 ppm and 7.31 ppm are formed by the coupling of H-3 with H-4, whereas the singlet signal at 8.08 ppm is attributed to H-6. In **2**, the singlet signals at 6.78 ppm and 9.09 ppm are attributed to the H-4 and H-6 aromatic protons. In **3** and **4**, the triplet signal 6.87 ppm and 6.82 ppm of H-5 are formed by the coupling with H-4 and H-6. The doublet signals at 7.24 ppm and 7.28 ppm for **3** as well as the doublet signals at 7.18 ppm and 7.41 ppm for **4** are formed by the coupling of H-5 with H-4 and H-6, respectively. The singlet signal from 11.30 ppm to 11.40 ppm is attributed to the proton of (N-NH). In the $^{13}$CNMR, the carbon signal at 147.88 ppm is attributed to the (C=N) group, the signal at 176.37 ppm is attributed to the carbon of the (C=S) goup, and the signal from 111.06 ppm to 146.64 ppm are attributed to aromatic carbons.

The complexes **1a–4a** exhibited well-resolved single crystals, FTIR spectra, $^{1}$H NMR, $^{13}$C NMR and elemental analysis results consistent with their assigned structures. In the FTIR, a two very sharp bands associated with (Mo=O) groups were observed from 893 $cm^{-1}$ to 944 $cm^{-1}$. In the $^{1}$H NMR spectra of ligands, the signals belonging to phenolic OH protons and N-NH protons are absent, whereas the signals belonging to the protons of the second ligand that occupies the D site are present, which is due to formation of the Mo complexes. The coordination-induced proton chemical shifts are most pronounced for the CS-NH proton, being upfield in all complexes. On the other hand, the CH=N proton is shifted downfield as a consequence of electron redistribution upon coordination with Mo. The complexes **1** and **3** in which the $CH_3OH$ molecule occupies the D site show a singlet signal at 3.18 ppm is attributed to the $CH_3$ protons. This signal is absent from the NMR spectra of the complexes **2** and **4** in which the D site occupied by $H_2O$ molecule. The complex **1a** showed different couplings between the aromatic protons compared to the ligand **1**. The doublet signal at 6.83 ppm is formed by the coupling of H-3 and H-4. The doublet of doublet signal of H-4 at 7.51 ppm is formed by the strong coupling with H-3 (J=9 Hz) and the weak coupling with H-6 (J=2.5 Hz) which show doublet signal at 7.48 ppm. These results are due to the conformational and geometrical changes upon coordination of 1 with *cis*-$MoO_2^{+2}$ core. In the $^{13}$C NMR spectra of ligands **1**-**4**, the signals belonging to the carbon of C=N and C=S groups are shifted up to 4 ppm and 18 ppm to upfield, upon complexation with Mo, respectively. This shielding effects are the sum induced shift and the formation of an imine bond in the complex instead of a thiocarbonyl C=S bond in the ligand. The complexes **1** and **3** show a signal at 48.56 ppm is attributed to the carbon of $CH_3$ group [23]. The data for all compounds are provided in the experimental section.

### 3.2. Crystal and molecular structures

Crystal and molecular structures of **1** and **4** and all the complexes were obtained using single crystal X-ray diffraction. The general crystal data for ligands and complexes are listed in Tables 1 and 2, the relevant bond distances and angles are shown in Tables 3 and 4, and their molecular structures are shown in Figs. 1–6.

The molecular structures of **1** and **4** (Figs. 1, 2) show the *trans* geometries of the S1 atom in relation to N1 and N2 atom in relation to C9 atom, as well as the *cis* geometries of S1 atom in relation to C9 atom and N1 atom in relation to N3 atom. In the free ligand, the C8–S1 bond length was 1.702(2) Å in **1** and 1.697(3) Å in **4**, whereas the N2–C8 bond length was 1.355(2) Å in **1** and 1.363(4) Å in **4**. These results indicate the tautomeric thione form of ligands. By contrast, the related molybdenum complexes **1a** (Fig.3) and **4a** (Fig. 6) show a meridional coordination plane that alters the C8–S1 bond length to 1.753(2) Å and 1.746(3) Å, as well as the N2–C8 bond length to 1.320(2) Å and 1.318(3) Å, respectively. These results indicate the tautomeric thiol form for the complexes.

In all complexes, the molybdenum atom has a distorted octahedral coordination. The ligand is bonded to the *cis*-$MoO_2^{+2}$ unit through the phenolate oxygen O1 or O4, the imine nitrogen N1, the thiolate sulfur S1, and an oxo group O3 lying *trans* to N1, whereas the other oxo group O2 (O4 in **1a**) lying *trans* to the D site occupied by $CH_3OH$ in **1a** and **3a** or $H_2O$ in **2a** and **4a**. Moreover, the complexes **1a** and **4a** show different geometries compared to their ligands **1** and **4**. The N1 atom is *cis* relative to S1 atom and *trans* relative to N3 atom. Meanwhile, the *trans* geometry between the C9 atom and N2 atom as well as the *cis* geometry between the S1 and C9 are unchanged during coordination the ligand **4** with $MoO_2^{+2}$ unit. Whereas, these geometries are changed during coordination the ligand 1 with $MoO_2^{+2}$ unit to *cis* and *trans*, respectively. The presence of $H_2O$ as a second ligand in **4a**, or $CH_3OH$ in **1a** are responsible for the geometry of the $MoO_2^{+2}$ surroundings that tend to increase the stability due to better electron delocalization in a chelated ring system that resulting from the

coordination with the metal center [24]. Accordingly, the complex **2a** show the same geometries of **4a**, whereas the complex 3a show the same geometries of **1a**.

The Mo–S distance ranging from 2.4204(5) Å in **1a** to 2.4574(3) Å in **2a**, Mo-N1 from 2.267(2) Å in **4a** to 2.298(2) Å in **1a** and the doubly bonded terminal oxo ligands ranging from 1.697(2) Å to 1.714(1) Å are responsible for the elongation of the Mo–D bond and the *trans* configuration of the O2 and O4 terminal oxo group [25].

### 3.3. Interaction with DNA

#### 3.3.1. Electronic absorption studies

Electronic absorption is one of the most useful methods in DNA binding studies [26, 27]. Complexes bind to DNA through covalent bonding by substituting the exchangeable ligand of the complexes with the nitrogen base of DNA [28] or noncovalent interaction, such as intercalation, electrostatic binding, or groove binding [29]. Absorption spectroscopic studies were carried out on a spectrophotometer (Perkin Elmer, Lambda-35), using fixed concentrations of the ligand or the complex (50 µM) with increasing amounts of DNA from 28.9 µM to 173.4 µM in 6.3 mM Tris-HCl/50 mM NaCl buffer (pH = 7). Each addition left for equilibrium at 25 °C for 10 min. and scanned from 230 nm to 600 nm. All the ligands and their complexes except **2** and its complex **2a** exhibited two absorption bands at 296 nm and 338 nm for **1a**, and at 305 nm and 338 nm for **3a** and **4a** which are attributed to the transitions $\pi$-$\pi^*$ and n-$\pi^*$, respectively. Both the ligand **2** and its complex **2a** exhibited one absorption band around 305 nm, which is attributed to $\pi$-$\pi^*$ transition. The $\pi$-$\pi^*$ absorption bands were used to monitor the interaction of CT DNA with ligands and complexes. All the ligands and their complexes showed a hypochromism with increasing DNA concentration (Fig. 7). The observed spectral behavior suggests intercalative binding to DNA, which leads to hypochromism in the spectral bands [26]. The change in absorbance values with increasing

amount of CT DNA were used to estimate the intrinsic binding constant $K_b$ at 298 nm for **2a** and, 305 nm for **1a**, **3a** and **4a** using an equation [30].

$$[DNA]/(\varepsilon_a - \varepsilon_f) = [DNA]/(\varepsilon_b - \varepsilon_f) + 1/K_b\,(\varepsilon_b - \varepsilon_f)$$

The absorption coefficients $\varepsilon_a$, $\varepsilon_f$, and $\varepsilon_b$ correspond to $A_{abs}/[DNA]$, the extinction coefficient for the free complex, and the extinction coefficient for the complex in fully bound form, respectively. The plot of $[DNA]/(\varepsilon_a - \varepsilon_f)$ versus [DNA] provided a slope $1/(\varepsilon_a - \varepsilon_f)$ and intercept $1/K_b\,(\varepsilon_b - \varepsilon_f)$ as shown in Fig. 8. The binding constants (Table 5) suggest that all the ligands and complexes bind to CT DNA. The complexes exhibit strong interaction compared to their related ligands, the highest $K_b$ value $6.318 \times 10^6$ $M^{-1}$ was observed for complex **1a**, whereas the lowest $k_b$ value was observed for complex **2a**. In addition, the binding of the complexes to CT DNA caused isosbestic spectral changes with an isosbestic points at 289 nm in the complexes **1a**, **3a** and **4a**. The complex **2a** show isosbestic spectral changes during the first four additions of CT DNA (28.9 μM to 115.6 μM) with the isosbestic point at 300 nm. The presence of isosbestic points at 289 nm are attributed to the increasing concentration of DNA which leads to increasing absorbance in this region [31].

3.3.2. Fluorescence emission studies

Emission spectral studies were carried out to know more on binding nature of the ligands and their Mo complexes to DNA. The fluorescence emission is due to return molecules to the electronic ground state π from the electronic excited state $\pi^*$ rather than the $n\rightarrow\pi^*$ transition because the quantum efficiency is greater and the lifetime is shorter than that for the $n\rightarrow\pi^*$ transition [32]. All the complexes showed fluorescence emission at 380 nm but the complexes of **1a** and **4a** showed a new peak at longer wavelength (500 nm) with isosbestic point at 408 nm, presumably due to formation of excimer (Fig. 9). This is attributed to the rigidity and steric features that succeed to bring the complex close enough for

excimer formation. The presence of bromine moiety on aromatic ring decreases the intensity of the monomeric fluorescent peak at 380 nm of **1a** which suggest that the probability of intersystem crossing increases depending on the molar mass of the halogen. By contrast, the presence of methyl moiety on aromatic ring increases the intensity of the monomeric fluorescent peak at 380 nm of **4a** due to increases the rigidity via the formation of hydrogen bonding [33]. As in Figure 1, the complexes of **2a** and **3a** show the decrease in fluorescence emission upon addition of CT-DNA which confirms the intercalative binding between the complexes and DNA. From the other hand, the CT-DNA addition to **1a** and **4a** lead to decreases the excimer fluorescent peaks at 500 nm and increases the monomeric fluorescent peaks at 380 nm. These changes are suggest to the intercalative interaction of excimer complex to DNA and hence separate the monomer complex which leads to rises the fluorescence intensity [34].

3.3.3. Viscosity measurement

Viscosity assays are regarded as one of the most important tests for assessing the binding modes of complexes to DNA. Intercalation of compounds into DNA increases the viscosity because of the extension and stiffening of the DNA helix [35]. The viscometric studies were performed by adding increasing amounts of the ligands and complexes to fixed amount of CT DNA at 37 °C in 6.3 mM Tris-HCl/50 mM NaCl buffer (pH = 7). The corresponding results are shown in Fig. 10. In general, the viscosity increases with the addition of ligand and complex. These results confirm the intercalative binding and support the spectrometric results.

3.4. DNA cleavage

Agarose gel electrophoresis of the pBR322 circular plasmid was used to investigate the effect of various microconcentrations of ligands and complexes (1.0 µM to 6.0 µM) on DNA cleavage. The assay was conducted in 6.3 mM Tris-HCl/50 mM NaCl buffer (pH= 7) in

the presence of a fixed amount (4.5 μM) of 30% $H_2O_2$ as an oxidant and incubated at 37 °C for 2 h. In Figure 11, lane 4 of the agarose gel electrophoresis reveals that all the ligands exhibit DNA cleavage in the plasmid DNA with the typical patterns of two forms, the fast migration form related to the closed circular supercoiled form (SC, form I) and the slow migration form related to the open circular relaxed form (OC, form II) [36]. The ligand **3** displayed significant cleavage of plasmid DNA, it nicked both the strands of plasmid DNA lead to show the linear form (form III) with disappearance of the SC form I (lanes 9 and 10). At highest concentration (6.0 μM), all the ligands inhibited the migration of the plasmid DNA (lane 11). On the other hand, the complexes exhibited higher cleavage activity on the plasmid DNA compared with that of the ligands. The complexes show the SC form I, the OC form II, and the linear form III. Interestingly, the complexes **1a** and **4a** exhibited three forms of cleavage at 4.0 μM (lanes 8), but SC form I disappeared when the concentration was increased to 4.5 μM (lanes 9). At 5.0 μM (lanes 10), the DNA lost its activity because of the inhibitory action of **1a** and **4a** at this concentration whereas the complex **2a** continued to show the OC and linear forms (lane 10), and then its inhibitory action on DNA migration was observed at 6.0 μM (lane 11). The significant cleavage activity on plasmid DNA also belong to the complex **3a**, which show the SC form I and linear form III at 3.0 μM (lane 6) and the plasmid DNA was totally converted into its linear form III at 3.5 μM (lane 7), and the inhibitory action of the complex was observed at 4.0 μM (lane 8).

All the agarose gel electrophoresis patterns show only the naturally occurring supercoiled form (SC, form I) for the DNA control and the buffer (lane 1), the DNA and ligand or complexes (lane 2), and the DNA, $H_2O_2$, and buffer (lane 3). This indicates that the activity of the ligands and complexes to cleave DNA occurs only in the presence of $H_2O_2$ as an oxidant (lanes 4–11) by the addition of a fixed amount (4.5 μM) of $H_2O_2$ to different amounts of ligand and complex (1 μM to 6 μM).

The activity to cleave DNA is greatly enhanced in complexes compared with the related free ligands, which indicates that the complexes produce hydroxyl radical from $H_2O_2$. This ability to generate hydroxyl radicals from metal ions is well reported [37, 38]. These free radicals contribute to the oxidation of deoxyribose moiety, followed by hydrolytic cleavage of the sugar phosphate backbone [39].

The results of DNA cleavage indicate that the location of substituents on the aromatic ring, the terminal N-aliphatic group and the second ligand occupied the coordination site (D) are essential role to DNA cleavage. The activity of these groups lies in to provide lipophilic properties, lead to enhance the affinity with hydrophobic medium of DNA.

3.5. Antitumor activity

Similar to the DNA binding and the DNA cleavage activity, the complexes demonstrated higher antiproliferative activity. The antiproliferation tests were performed *in vitro* on the human colorectal cancer cell line HCT 116. The complexes exhibited more pronounced activity than the standard reference 5-fluorouracil ($IC_{50}$ = 7.3 µM). The median inhibitory concentrations ($IC_{50}$) of the tested compounds are given in Table 5. The results show that the antiproliferative efficiency depends on the substituent on the aromatic ring and the group of the site D. The complexes **1a** and **3a** with the $CH_3OH$ at the site D showed more activity than the complexes **2a** and **4a** with an $H_2O$ molecule at the site D. Moreover, the results also reveal that the complex **1a** ($IC_{50}$ = 3.3 µM) is somewhat active than **3a** ($IC_{50}$ = 3.5 µM), whereas the complex **4a** ($IC_{50}$ = 4.0 µM) is active than the complex **2a** ($IC_{50}$ = 5.0 µM). These results justify the importance of substituents in aromatic ring on antiproliferation efficiency, which were in the following order Br ~ $C(CH_3)_3$ > $CH_3$ > $CH_2$-CH=$CH_2$, $OCH_3$. These results are consistent with the binding capabilities of the complexes with CT DNA, except for some narrow differences in $IC_{50}$ and $K_b$ between **1a** and **3a**. Furthermore, the

percentage inhibition of cell proliferation using six selected concentration of complexes (3, 6, 12, 25, 50, and 100 μM) (Fig. 12) show inhibitory activity at 100 μM in the order **1a** ~ **3a** > **4a** > **2a**, at 96.6%, 96.2%, 85.9%, and 58.6%, respectively. Figure 13 shows the photomicrographs of HCT 116 cells after 48 h treatment with the complexes. These images were taken under an inverted phase-contrast microscope at ×200 magnification using a digital camera at 48 hours after treatment with the samples. The photomicrograph of the untreated (control) group show aggressively growing cells at full confluence and the compact monolayer of HCT 116 cells. Closer inspection of these images of untreated and treated cells clearly demonstrate the strong cytotoxicity of the complexes against human colorectal (HCT 116) cells. The analysis of photomicrographs shows that the complexes generally cause apoptotic features in the affected cells. The blebbing of the cell membrane, nuclear condensation, and formation of vesicles in the treated cells clearly indicate the distinct characteristics of apoptosis.

## 4. Conclusions

The synthesis, structural description, and biological evaluation of the four molybdenum(VI) complexes **1a**–**4a** have been studied. The complexes show that thiosemicarbazonato ligands **1**–**4** are coordinated to molybdenum as tridentate ONS-donors. According to the X-ray crystallography results, the complexes exhibit distorted octahedral coordination. The complexes efficiently binds to CT DNA, as indicated by the high binding constant $K_b$, ranging from $7.486 \times 10^5$ $M^{-1}$ to $6.318 \times 10^6$ $M^{-1}$, the UV hypochromism of the absorption bands, the increase in viscosity with increasing CT DNA concentration, and the efficient cleavage of the plasmid pBR 322 DNA. In general, the complexes exhibit higher activity than their respective ligands.

The antiproliferative activity of the complexes was investigated against human colorectal (HCT 116) cell line. All the complexes show high *in vitro* anticancer activities in relative order **1a** ~ **3a** > **4a** > **2a** according their $IC_{50}$ values; 3.3, 3.5, 4.0, and 5.0 μM respectively.

**Acknowledgements**

We thank the Universiti Sains Malaysia and the Malaysian Government for a Research Grant which partly supported this work.

**Supplementary material**

CCDC 890717 and 931644 contain the supplementary data for **1** and **4**. CCDC 888002, 893000, 902961, and 905155 contain the supplementary data for **1a**, **2a**, **3a**, and, **4a**, respectively. These data can be obtained free of charge at http://www.ccdc.cam.ac.uk/data_request/cif.

**References**

[1] D. Kovale-Demertzi, D. Domopoulou, M. Demertzis, C.P. Raptopoulou, A. Terzis, Polyhedron 13(1994) 1917-1925

[2] R. Finch, M. Liu, A. Cory, J. Cory, A. Sartorelli, Adv Enzyme Regul 39 (1999) 3-12.

[3] P.I.da S. Maia, F.R. Pavan, C.Q.F. Leite, S.S. Lemos, G.F. de Sousa, A.A. Batista, O.R. Nascimento, J. Ellena, E.E. Castellano, E. Niquet, V.M. Deflon, Polyhedron 28 (2009) 398-406.

[4] F. R. Pavan, P. I.da S. Maia, S.R.A. Leite, V.M. Deflon, A.A. Batista, D.N. Sato, S.G. Franzblau, C.Q.F. Leite, Eur. J. Med. Chem. 45 (2010) 1898-1905.

[5] X. Du, C. Guo, E. Hansall, P.S. Doyle, C.R. Caffrey, T.P. Holler, J.H. McKerrov, F.E. Cohen, J.Med. Chem. 45 (2002) 2695- 2707.

[6] D. B. Lovejoy, D.R. Richardson, Blood 100 (2002) 666- 676.

[7] A.E. Liberta, D.X. West, Biometals 5 (1992) 121-126.

[8] M. Belicchi-Ferrart, F. Bisceglie, C. Casoli, S. Durot, I. Morgenstern-Badarau, G. Pelosi, E. Pilotti, S. Pinelli, P. Tarasconi, J. Med. Chem. 48 (2005) 1671-1675.

[9] Z. Afrasiabi, E. Sinn, J. Chen, Y. Ma, A. L. Rheingold, L. N. Zakharov, N. Rath . S. Padhye, Inorg. Chim. Acta 357 (2004) 271-278.

[10] R. R. Mrndel, F. Bittner, Biochim. Biophys. Acta Mol. Cell Res 1763 (2006) 621- 635 .

[11] C. D. Brondino, M. J. Romao, I. Moura, J.J.G. Moura, Curr. Opin. Chem.Biol. 10 (2006) 109-114.

[12] G. Hou , R. Dick, C. Zeng, G. J.Brewer, Transl. Res. 149 (2007) 260-264.

[13] B. Hassouneh, M. Islam, T. Nagel, Q. Pan, S.D. Merajver, T.N. Teknos, Mol. Cancer Ther. 6 (2007) 1039-1045.

[14] A. Rana, R. Dinda, P. Sengupta, L. R. Falvello, S. Ghosh, Polyhedron 21(2002) 1023-1030.

[15] C. Bustos, O. Burckhardt, R. Schrebler, D. Carrillo, A.M. Arif, A.H. Cowley, C.M. Nunn, Inorg.Chem. 29 (1990) 3996-4001.

[16] J. Liimatainen, A. Lehtonen, R. Sillanpaa, Polyhedron 19 (2000) 1133-1138.

[17] G.M. Sheldrick, Acta Cryst. A64 (2008) 112-122.

[18] M.E. Reichmann, S.A. Rice, C.A. Thomas, P. Doty, J. Am. Chem. Soc. 76 (1954) 3047-3053.

[19] G. Cohen, H. Eisenberg, Biopolymers 8 (1969) 45-55.

[20] T. Mosmann, J. Immunol. Methods 65 (1983) 55-63.

[21] V. Vrdoljak, M. Cindric, D. Milic, D. Matkovic-Calogovic, P. Novak, B. Kamenar, Polyhedron 24 (2005) 1717-1726.

[22] N. K. Ngan, K.M. Lo, C.S.R. Wong, Polyhedron 33 (2012) 235-251.

[23] V. Vrdoljak, M. Cindric, D. Matkovic-Calogovic, B. Prugovecki, P. Novak, B. Kamenar, Z. Anorg. Allg. Chem. **631** (2005) 928-936.

[24] L. Coghi, A. M. M. Lanfredi, A. Tiripicchio, J. Chem. Soc., Perkin Trans. 2 (1972)1808-1810.

[25] D. Eierhoff, W. C. Tung, A. Hammerschmidt, B. Krebs, Inorg. Chim. Acta 362 (2009) 915-928.

[26] J. K. Barton, A.T. Danishefsky, J.M. Goldberg, J. Am. Chem. Soc. 106 (1984) 2172- 2176.

[27] H. Chao, W. Mei, Q. Huang, L. Ji, J. Inorg. Biochem. 92 (2002) 165-170.

[28] S.E. Sherman, D. Gibson, A.H.J. Wang, S.J. Lippard, J. Am. Chem. Soc.110 (1988) 7368-7381.

[29] L. Strekowski, B. Wilson, Mutat. Res. 623 (2007) 3-13.

[30] A. Wolfe, G.H. Shimer, T. Meehan, Biochemistry 26 (1987) 6392-6396.

[31] M. Jamil, A. A. Altaf, A. Badshah, Shafiqullah, I. Ahmad, M. Zubair, S. Kemal, M. I. Ali, Spectrochim. Acta A 105 (2013) 165-170.

[32] . A. Skoog, F. J. Holler, S. R. Crouch, Principles of Instrumental Analysis, 6th edition, Thomson Brooks/Cole, 2007.

[33] D. C. Harris, M. D. Bertolucci, Symmetry and Spectroscopy: An Introduction to Vibrational and Electronic Spectroscopy, Dover Publications, Inc., New York, 1989.

[34] ] Z. Xu, N. J. Singh, J. Lim, J. Pan, H. N. Kim, S. Park, K. S. Kim, J. Yoon, J. Am. Chem. Soc., 131 (2009) 15528-15533.

[35] S. Satyanarayana, J.C. Dabrowiak, J.B. Chaires, Biochemistry 31 (1992) 9319-9324.

[36] E.J. Gao, M.C. Zhu, Y. Huang, L. Liu, F.C. Liu, S. Ma, C.Y. Shi, Eur. J. Med. Chem. 45(2010) 1034-1041.

[37] L.E. Marshall, D.R. Graham, K.A. Reich, D.S. Sigman, Biochemistry 20 (1981) 244-250.

[38] C. Walling, Acc. Chem. Res. 8(1975) 125-131.

[39] W.K. Pogozelski, T.D. Tullius, Chem.Rev. 98 (1998) 1089-1107.

**Figure captions**

**Scheme 1.** General synthetic procedure of ligands and complexes

**Fig. 1.** Molecular structure of **1**

**Fig. 2.** Molecular structure of **4**

**Fig. 3.** Molecular structure of **1a**

**Fig. 4.** Molecular structure of **2a**

**Fig. 5.** Molecular structure of **3a**

**Fig. 6.** Molecular structure of **4a**

**Fig. 7.** UV spectra of complexes **1a**- **4a** in 6.3 mM Tris-HCl/50 mM NaCl buffer (pH= 7) in presence of CT DNA at increasing amounts.[complex] = 50 µM , [DNA] = (28.9 - 173.4) µM . The arrows show the changes in absorbance upon increasing amounts of CT DNA.

**Fig. 8.** Plots of $[DNA]/(\varepsilon_a - \varepsilon_f)$ vs [DNA].

**Fig. 9.** Fluorescence spectra of complexes **1a**- **4a** in 6.3 mM Tris-HCl/50 mM NaCl buffer (pH= 7) in presence of CT DNA at increasing amounts.[complex] = 50 µM , [DNA] = (28.9 - 173.4) µM.The arrows show the changes in fluorescence intensity upon increasing amounts of CT DNA.

**Fig. 10.** Viscometric results of ligands (A) and complexes (B) , in 6.3 mM Tris-HCl/50 mM NaCl buffer (pH= 7) in presence of CT DNA at increasing amounts of ligand/complex at 37 $^0$C.

**Fig. 11.** Agarose gel electrophoresis patterns of pBR 322 (0.025 µM) increasing concentrations (1.0 µM – 6.0 µM) of ligands **1**- **4** and complexes **1a**- **4a** in 6.3 mM Tris-HCl/50 mM NaCl buffer (pH= 7) incubated at 37 $^0$C for 2h , using $H_2O_2$ (4.5 µM) and ladder 1 KbDNA as a marker (lane L); lane 1, pBR 322 DNA ; lane 2, DNA + Sample (ligand or complex)(6 µM); lane 3, DNA+ $H_2O_2$ ; lane 4, DNA +$H_2O_2$+ Sample (1 µM);lane 5, DNA +$H_2O_2$+ Sample(2 µM); lane 6, DNA +$H_2O_2$+ Sample (3 µM); lane 7 , DNA +$H_2O_2$+ Sample(3.5 µM); lane 8, DNA +$H_2O_2$+ Sample(4 µM); lane 9, DNA +$H_2O_2$+ Sample(4.5 µM); lane 10, DNA +$H_2O_2$+ Sample (5 µM); lane 11, DNA +$H_2O_2$+ Sample(6 µM).

**Fig. 12.** Cell proliferation inhibition by complexes in concentration range 3.0-100 µM using 5-FU as a reference.

**Fig. 13.** Photomicrographs of the HCT 116 cell lines before and after treatment with complexes ; image control = proliferation cells before treatment , the images after treatment for **1a**- **4a** and 5-FU= standard reference.

**Table 1**

Crystallographic data for ligands **1** and **4**

| | **1** | **4** |
|---|---|---|
| Chemical formula | $C_{10}H_{12}BrN_3OS$ | $C_{11}H_{15}N_3OS$ |
| Formula weight | 302.20 | 237.33 |
| Crystal system | monoclinic | Triclinic |
| Crystal description | block yellow | block colorless |
| Space group | C2/c | P-1 |
| *Unit cell dimensions* | | |
| $a$ ($A^0$) | 22.0348(5) | 6.6812(5) |
| $b$ ($A^0$) | 11.8148(3) | 9.4891(7) |
| $c$ ($A^0$) | 9.5016(2) | 10.6380(8) |
| $\alpha$ ($^0$) | 90 | 76.720(5) |
| $\beta$ ($^0$) | 101.781(1) | 74.327(5) |
| $\gamma$ ($^0$) | 90 | 69.978(5) |
| Volume ($^0A^3$) | 2421.51(10) | 603.05(8) |
| Z | 8 | 2 |
| $D_{calc}$ (g/cm$^3$) | 1.658 | 1.307 |
| Crystal size (mm) | 0.21 x 0.29 x 0.52 | 0.11 x 0.31 x 0.33 |
| Temperature (K) | 100 | 100 |
| Total data | 16916 | 9105 |
| Unique data | 4414 | 3176 |
| $R_{int}$ | 0.019 | 0.058 |
| Observed data [I>2σ(I)] | 3568 | 2372 |
| $R_1$ | 0.0304 | 0.0318 |
| $wR_2$ | 0.0748 | 0.0755 |
| S | 1.06 | 1.05 |

**Table 2**

Crystallographic data for complexes **1a**- **4a**

| | **1a** | **2a** | **3a** | **4a** |
|---|---|---|---|---|
| Chemical formula | $C_{11}H_{14}BrMoN_3O_4S$, $CH_3O$ | $C_{14}H_{19}MoN_3O_5S$ | $C_{14}H_{21}MoN_3O_4S$ | $C_{11}H_{13}MoN_3O_4S$ |
| Formula weight | 491.20 | 437.33 | 423.35 | 379.25 |
| Crystal system | triclinic | triclinic | monoclinic | monoclinic |
| Crystal description | block orange | block red | block brown | plate orange |
| Space group | P-1 | P-1 | P21/c | P21/c |
| *Unit cell dimensions* | | | | |
| $a$ ($A^0$) | 7.5639(1) | 8.3916(1) | 7.8445(1) | 10.0623(3) |
| $b$ ($A^0$) | 9.4661(2) | 9.9128(2) | 16.7335(3) | 8.1658(2) |
| $c$ ($A^0$) | 12.3666(2) | 10.2619(2) | 13.5415(2) | 17.5959(5) |
| $\alpha$ ($^0$) | 78.853(1) | 90.527(1) | 90 | 90 |
| $\beta$ ($^0$) | 75.665(1) | 96.753(1) | 103.663(1) | 100.765(2) |
| $\gamma$ ($^0$) | 85.795(1) | 95.854(1) | 90 | 90 |
| Volume ($^0A^3$) | 841.40(3) | 843.09(3) | 1727.24(5) | 1420.35(7) |
| Z | 2 | 2 | 4 | 4 |
| $D_{calc}$ ($g/cm^3$) | 1.939 | 1.723 | 1.628 | 1.816 |
| Crystal size (mm) | 0.20 x 0.29 x 0.43 | 0.08 x 0.20 x 0.28 | 0.13 x 0.14 x 0.39 | 0.10 x 0.17 x 0.40 |
| Temperature (K) | 100 | 100 | 100 | 100 |
| Total data | 22374 | 29389 | 23091 | 14593 |
| Unique data | 6082 | 8116 | 6279 | 4128 |
| $R_{int}$ | 0.023 | 0.022 | 0.028 | 0.039 |
| Observed data [I>2σ(I)] | 5635 | 7463 | 5344 | 3494 |
| $R_1$ | 0.0230 | 0.0232 | 0.0389 | 0.0276 |
| $wR_2$ | 0.0699 | 0.0592 | 0.0838 | 0.0767 |
| S | 1.12 | 1.06 | 1.13 | 1.11 |

**Table 3**

Selected bond length ($A^0$) for the **1**, **2** and the complexes **1a – 4a**

| | 1 | 2 | | 1a | 2a | 3a | 4a |
|---|---|---|---|---|---|---|---|
| S1-C8 | 1.7019(15) | 1.697(3) | Mo1-S1 | 2.4204(5) | 2.4574(3) | 2.4339(6) | 2.4514(7) |
| N2-C8 | 1.355(2) | 1.363(4) | Mo1-O1 | 1.9361(13) | 1.9501(8) | 2.3202(17) | 1.9722(19) |
| N3-C8 | 1.326(2) | 1.326(4) | Mo1-O2 | 2.3091(13) | 1.7018(9) | 1.6967(16) | 1.697(2) |
| C6-C7 | 1.453(2) | 1.454(4) | Mo1-O3 | 1.7071(13) | 1.7110(9) | 1.7137(16) | 1.7120(17) |
| N1-C7 | 1.290(2) | 1.287(4) | Mo1-O4 | 1.7048(14) | 2.2476(9)[a] | 1.9256(15) | 2.277(2) |
| C5-C6 | 1.405(2) | 1.405(5) | Mo1-N1 | 2.2982(14) | 2.2869(9) | 2.2793(18) | 2.267(2) |
| O1-C1 | 1.3521(19) | 1.362(4) | | | | | |
| N1-N2 | 1.3833(19) | 1.379(4) | | | | | |

[a] O4=O1W

**Table 4**

Selected angles ( $^0$ ) of the complexes

| | 1a | 2a | 3a | 4a |
|---|---|---|---|---|
| S1-Mo1-O1 | 153.75(4) | 153.03(3) | 81.77(5) | 153.71(6) |
| S1-Mo1-O2 | 81.99(3) | 97.04(3) | 97.18(6) | 98.03(7) |
| S1-Mo1-O3 | 90.18(5) | 92.12(3) | 90.74(5) | 91.59(7) |
| S1-Mo1-O4 | 97.28(5) | 82.28(2)[a] | 153.27(5) | 82.40(5) |
| S1-Mo1-N1 | 76.27(4) | 75.83(2) | 75.69(5) | 76.11(6) |
| O1-Mo1-O2 | 78.40(5) | 97.75(4) | 169.80(7) | 97.89(8) |
| O1-Mo1-O3 | 104.92(6) | 105.38(4) | 84.68(7) | 103.92(8) |
| O1-Mo1-O4 | 99.12(6) | 78.78(3)[a] | 78.76(6) | 8.42(7) |
| O1-Mo1-N1 | 82.77(5) | 82.11(3) | 76.23(6) | 82.59(8) |
| O2-Mo1-O3 | 84.22(6) | 105.63(4) | 105.50(8) | 105.99(9) |
| O2-Mo1-O4 | 170.29(6) | 168.53(4)[a] | 98.74(7) | 170.19(8) |
| O2-Mo1-N1 | 78.35(5) | 88.62(4) | 93.66(7) | 91.86(9) |
| O3-Mo1-O4 | 105.48(7) | 85.84(4)[a] | 105.42(7) | 83.78(8) |
| O3-Mo1-N1 | 159.17(6) | 162.52(4) | 157.86(7) | 159.70(9) |
| O4-Mo1-N1 | 92.05(6) | 80.09(3)[a] | 81.98(6) | 78.69(7) |

[a] O4=O1W

**Table 5**

$IC_{50}$ (µM) values for the complexes and DNA binding constants ($K_b$) for the ligands and complexes

| Ligand | $K_b$ ($M^{-1}$) | Complex | $K_b$($M^{-1}$) | $IC_{50}$(µM) |
|---|---|---|---|---|
| **1** | $2.888 \times 10^{5}$ | **1a** | $6.318 \times 10^{6}$ | 3.3 |
| **2** | $8.298 \times 10^{4}$ | **2a** | $7.486 \times 10^{5}$ | 5.0 |
| **3** | $1.834 \times 10^{5}$ | **3a** | $5.552 \times 10^{6}$ | 3.5 |
| **4** | $9.052 \times 10^{4}$ | **4a** | $8.791 \times 10^{5}$ | 4.0 |
| | | **5-FU** | | 7.3 |

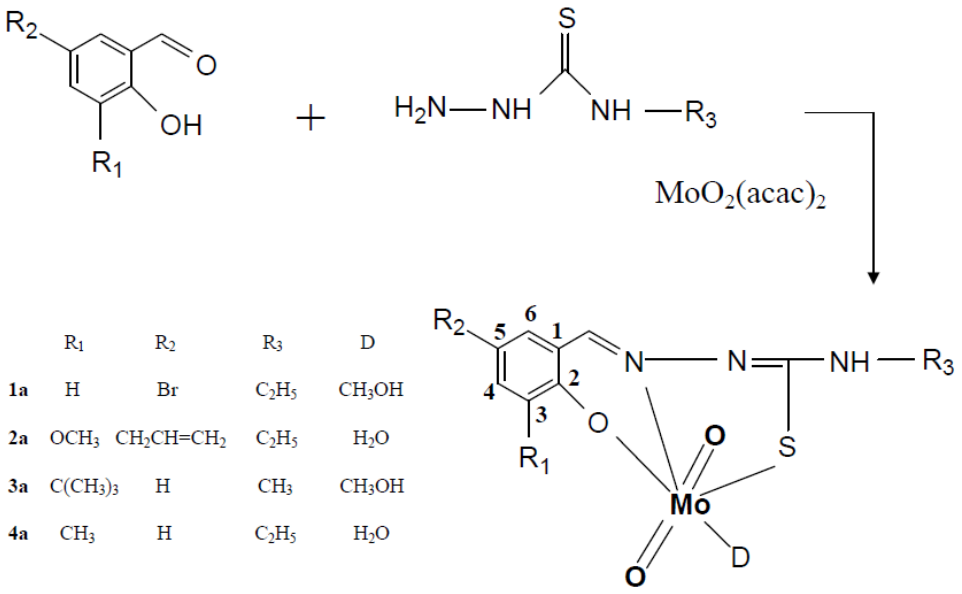


| | $R_1$ | $R_2$ | $R_3$ | D |
|---|---|---|---|---|
| **1a** | H | Br | $C_2H_5$ | $CH_3OH$ |
| **2a** | $OCH_3$ | $CH_2CH{=}CH_2$ | $C_2H_5$ | $H_2O$ |
| **3a** | $C(CH_3)_3$ | H | $CH_3$ | $CH_3OH$ |
| **4a** | $CH_3$ | H | $C_2H_5$ | $H_2O$ |

**Scheme 1.** General synthetic procedure of ligands and complexes

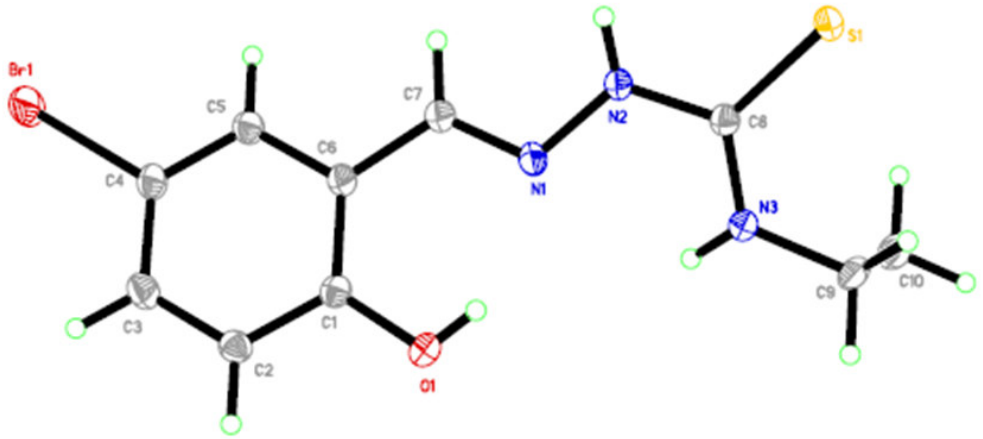


**Fig. 1.** Molecular structure of **1**

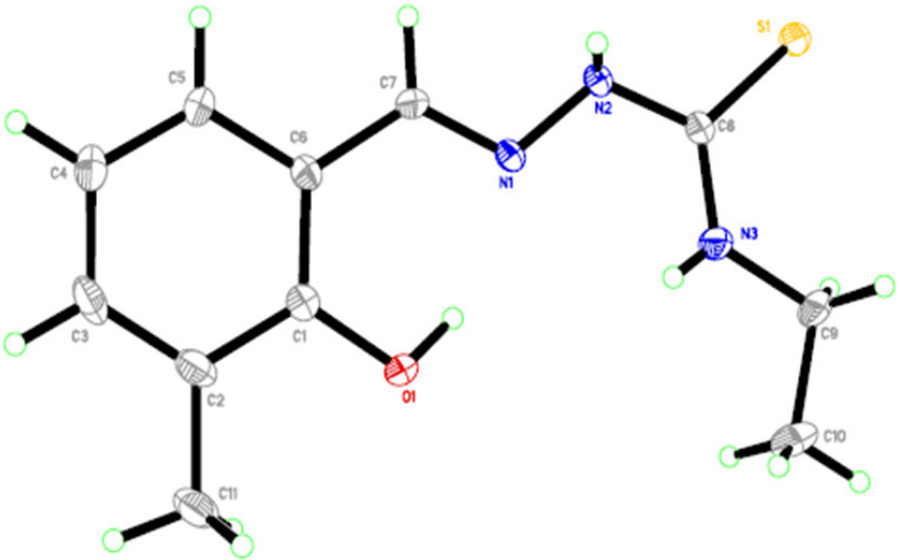


**Fig. 2.** Molecular structure of

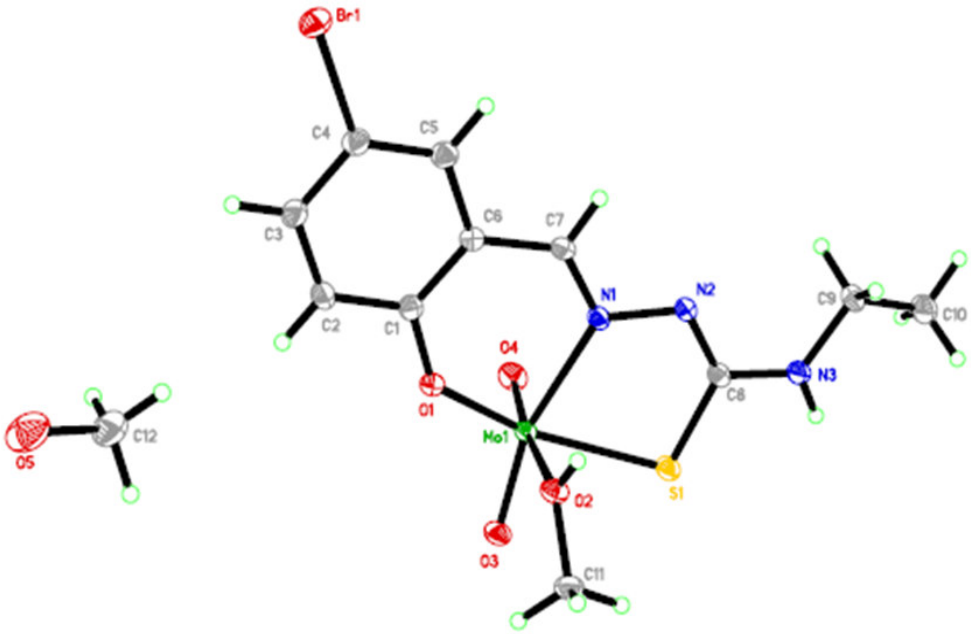


**Fig. 3.** Molecular structure of **1a**

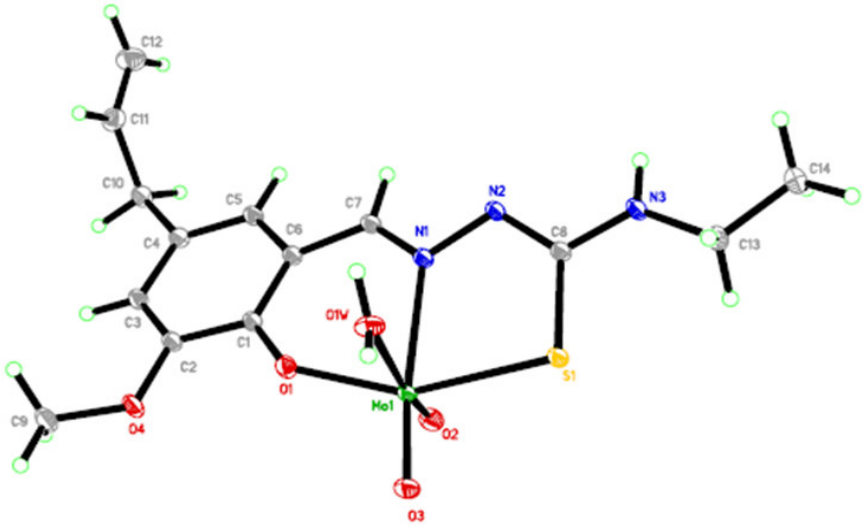


**Fig. 4.** Molecular structure of **2a**

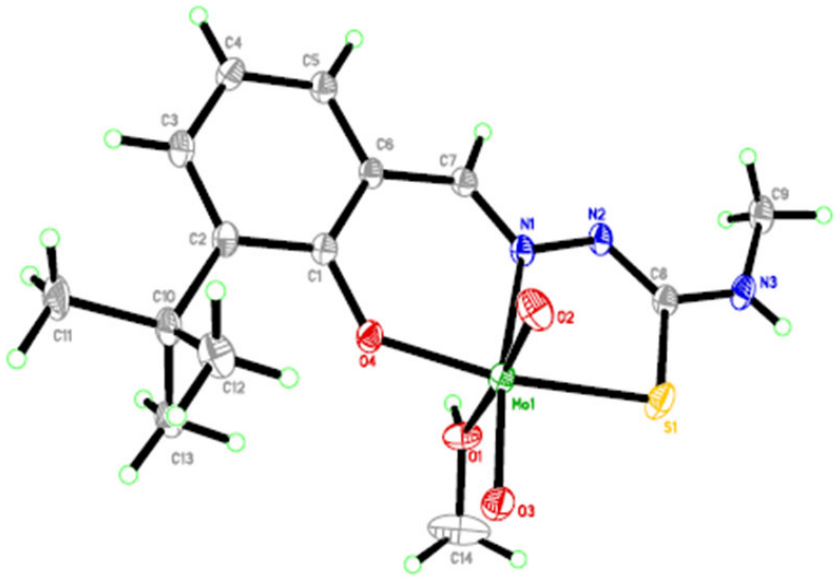


**Fig. 5.** Molecular structure of **3a**

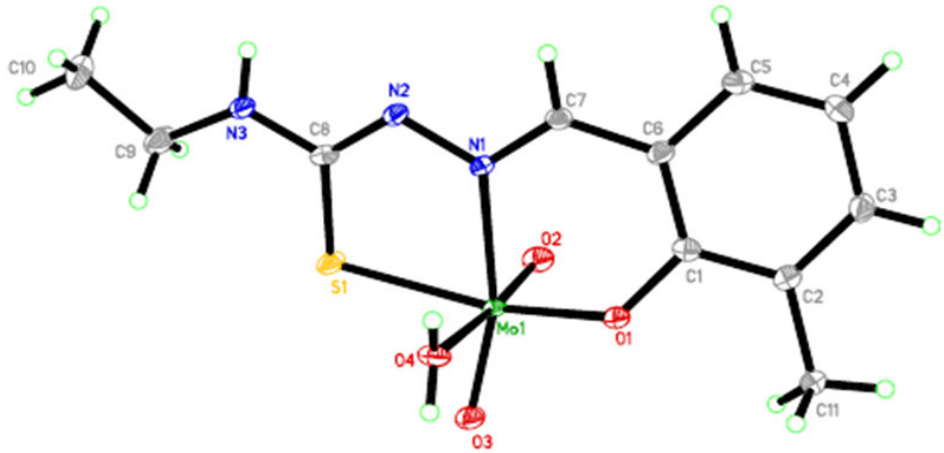


**Fig. 6.** Molecular structure of **4a**

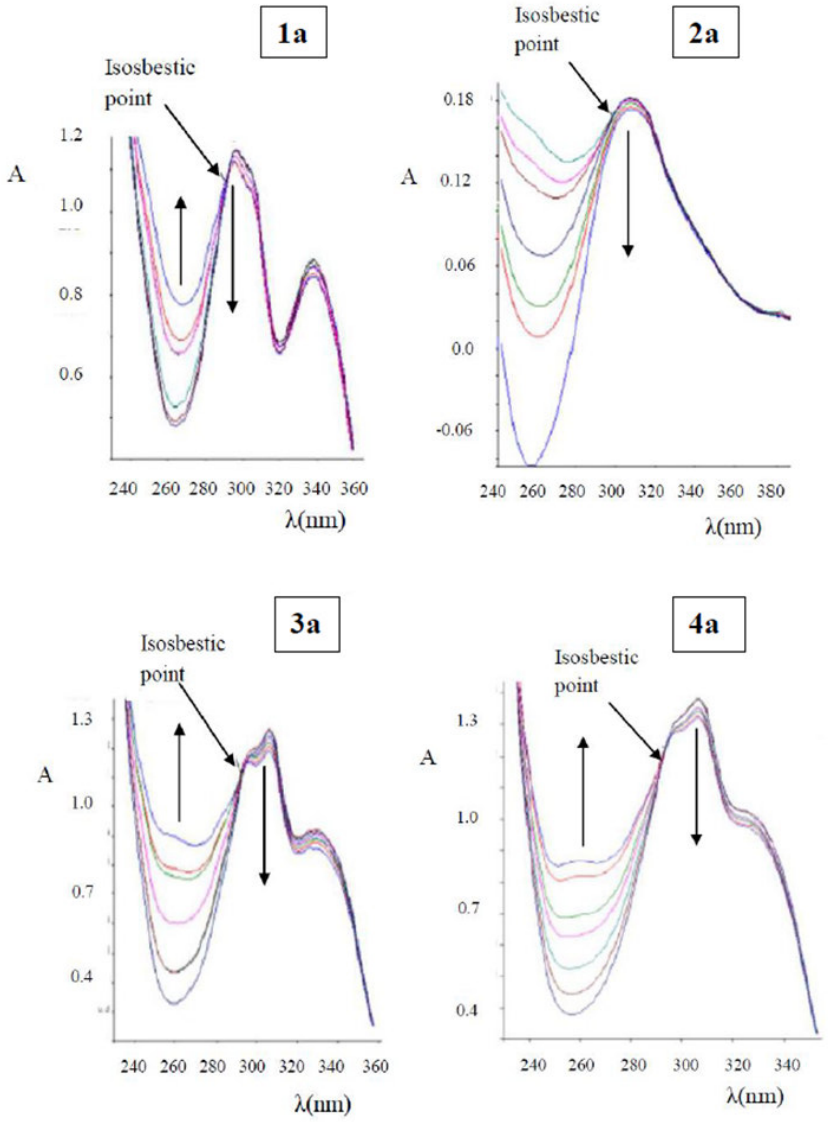


**Fig. 7.** UV spectra of complexes **1a**- **4a** in 6.3 mM Tris-HCl/50 mM NaCl buffer (pH= 7) in presence of CT DNA at increasing amounts.[complex] = 50 µM , [DNA] = (28.9 - 173.4) µM . The arrows show the changes in absorbance upon increasing amounts of CT DNA.

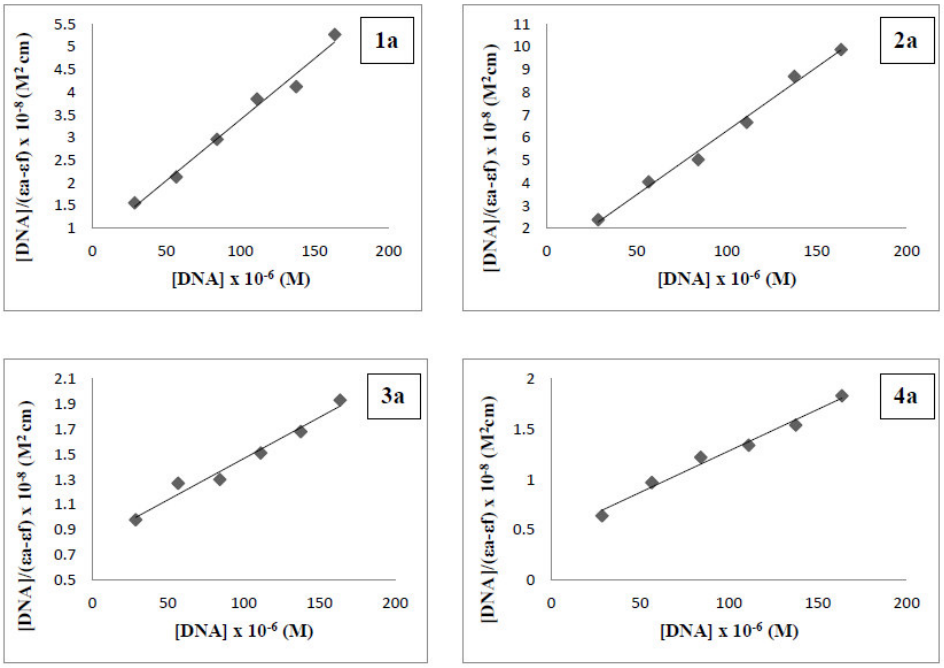


**Fig. 8.** Plots of $[DNA]/(\varepsilon_a - \varepsilon_f)$ vs [DNA].

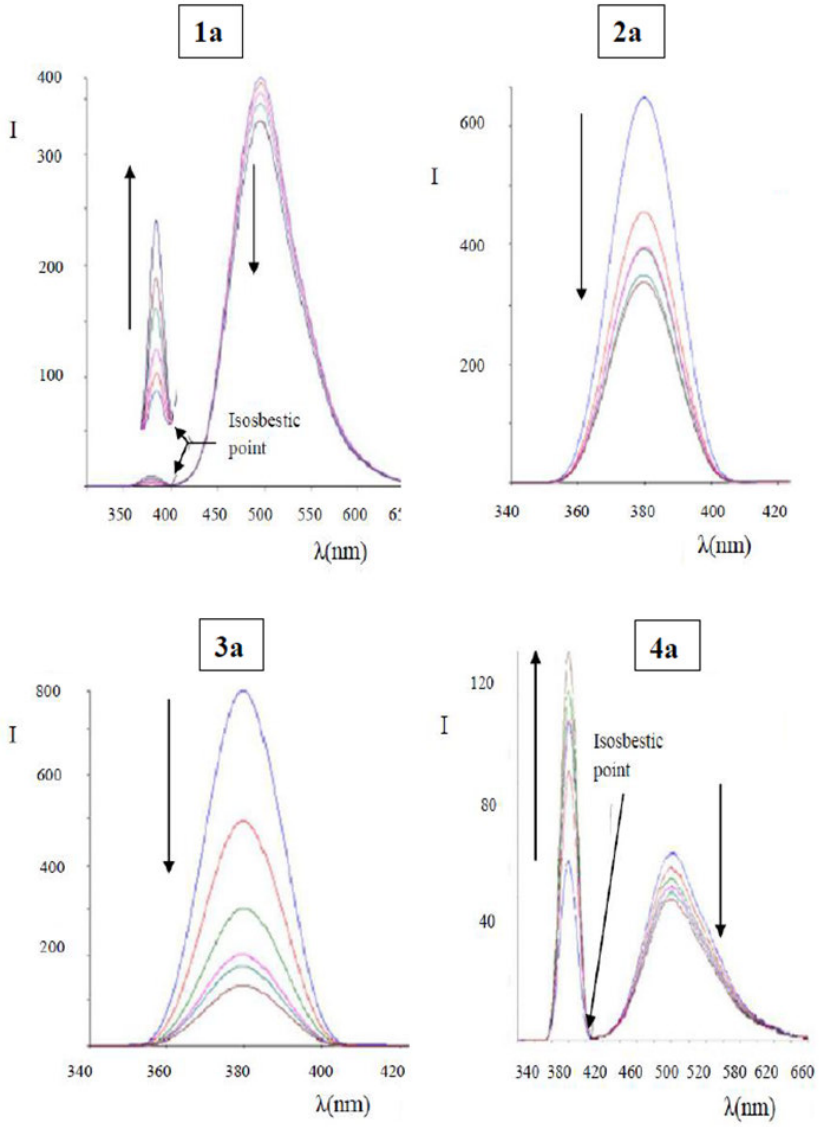


**Fig. 9.** Fluorescence spectra of complexes **1a**- **4a** in 6.3 mM Tris-HCl/50 mM NaCl buffer (pH= 7) in presence of CT DNA at increasing amounts.[complex] = 50 µM , [DNA] = (28.9 - 173.4) µM.The arrows show the changes in fluorescence intensity upon increasing amounts of CT DNA.

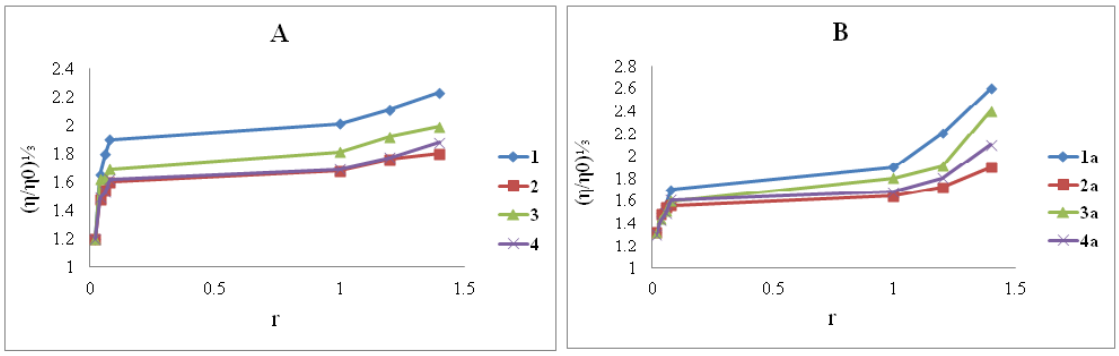


**Fig. 10.** Viscometric results of ligands (A) and complexes (B) in 6.3 mM Tris-HCl/50 mM NaCl buffer (pH= 7) in presence of CT DNA and increasing amounts of ligand/complex at 37 $^{0}$C.

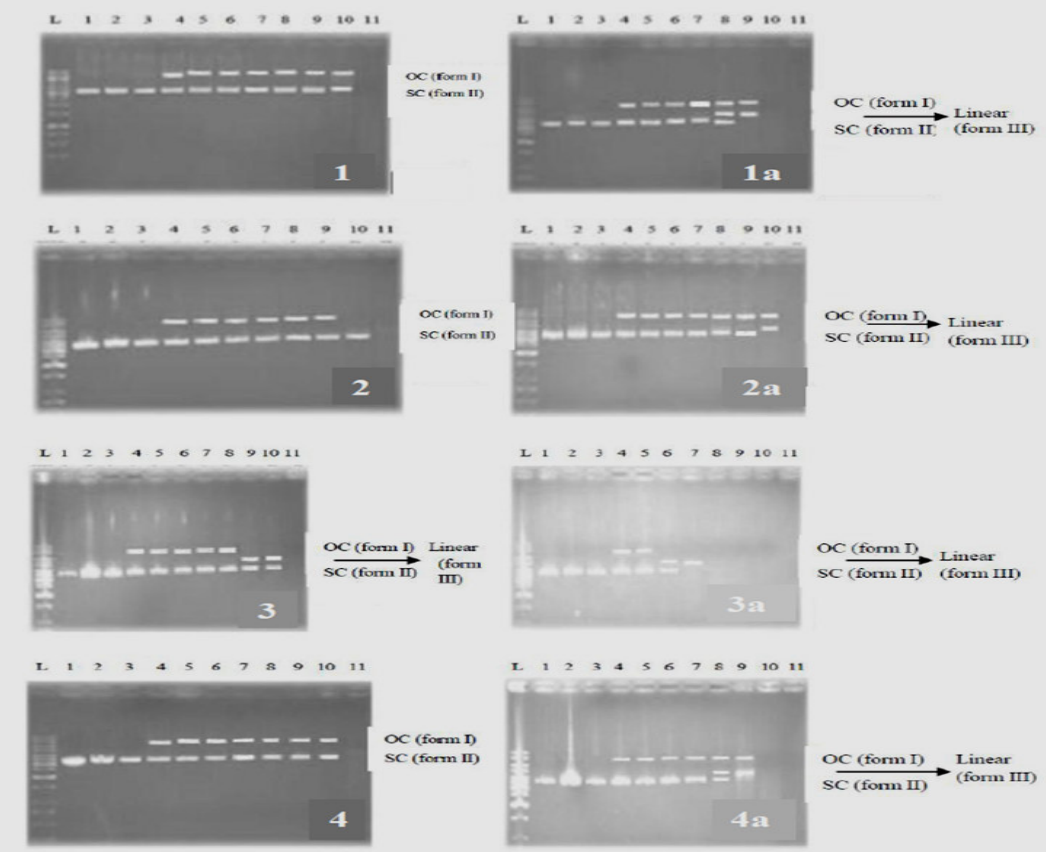


**Fig. 11.** Agarose gel electrophoresis patterns of pBR 322 (0.025 µM) increasing concentrations (1.0 µM – 6.0 µM) of ligands **1**- **4** and complexes **1a**- **4a** in 6.3 mM Tris-HCl/50 mM NaCl buffer (pH= 7) incubated at 37 $^{0}$C for 2h , using $H_2O_2$ (4.5 µM) and ladder 1 KbDNA as a marker (lane L); lane 1, pBR 322 DNA ; lane 2, DNA + Sample (ligand or complex)(6 µM); lane 3, DNA+ $H_2O_2$ ; lane 4, DNA +$H_2O_2$+ Sample (1 µM);lane 5, DNA +$H_2O_2$+ Sample(2 µM); lane 6, DNA +$H_2O_2$+ Sample (3 µM); lane 7 , DNA +$H_2O_2$+ Sample(3.5 µM); lane 8, DNA +$H_2O_2$+ Sample(4 µM); lane 9, DNA +$H_2O_2$+ Sample(4.5 µM); lane 10, DNA +$H_2O_2$+ Sample (5 µM); lane 11, DNA +$H_2O_2$+ Sample(6 µM).

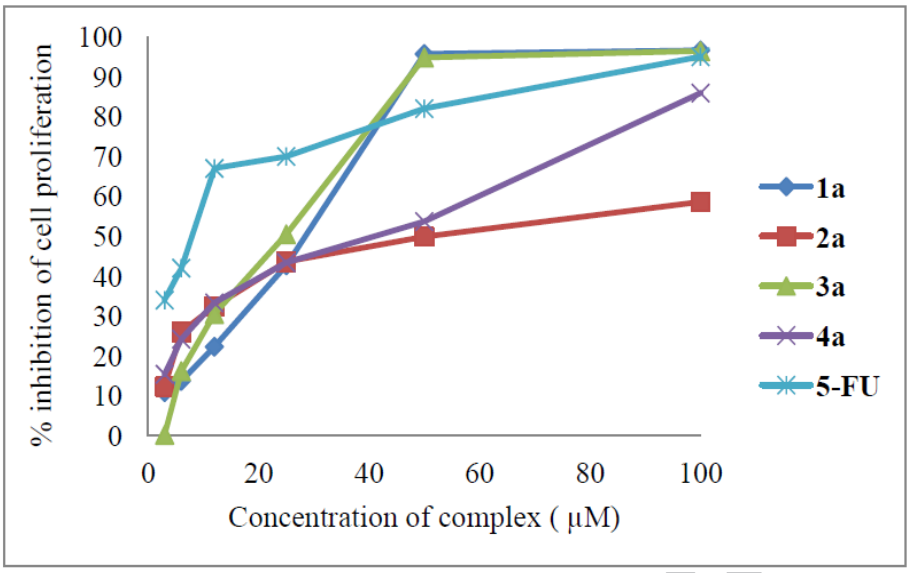


**Fig. 12.** Cell proliferation inhibition by complexes in concentration range 3.0-100 µM using 5-FU as a reference.

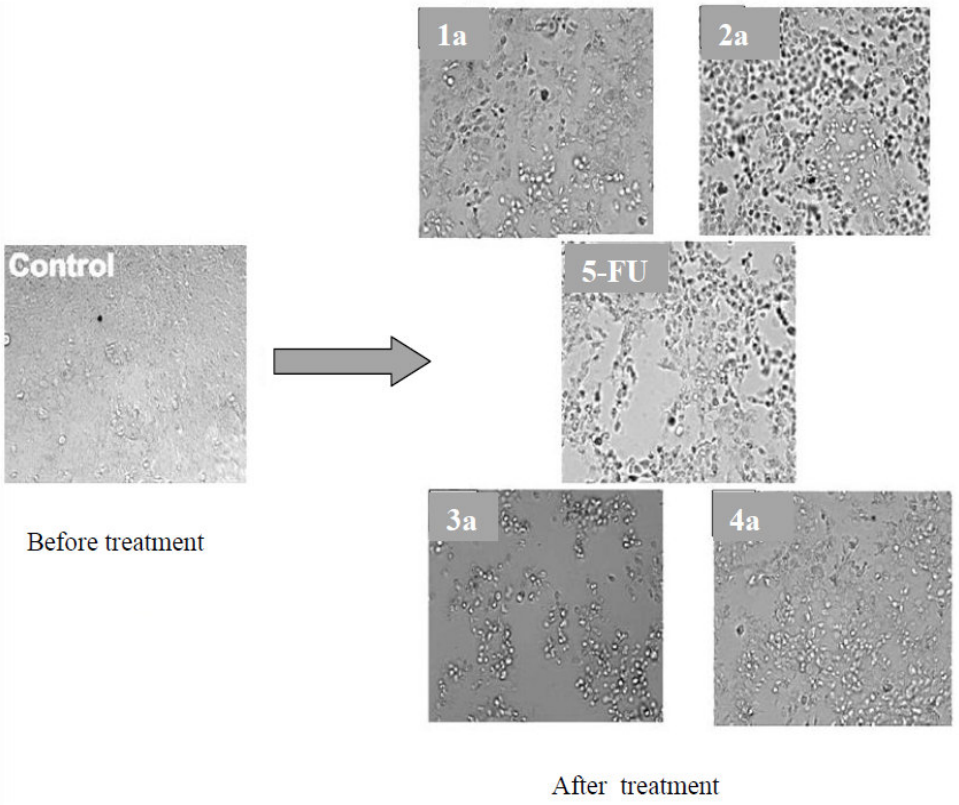


**Fig. 13.** Photomicrographs of the HCT 116 cell lines before and after treatment with complexes ; image control = proliferation cells before treatment , the images after treatment for **1a**- **4a** and 5-FU= standard reference.

**Mononuclear dioxomolybdenum(VI) thiosemicarbazonato complexes : Synthesis, characterization, structural illustration, *in vitro* DNA binding, cleavage, and antitumor properties**

**Mouayed A. Hussein [a] , Teoh S. Guan [a *], Rosenani A. Haque [a] , Mohamed B. Khadeer Ahamed[b], Amin M.S. Abdul Majid[b]**

[a] School of Chemical Science , Universiti Sains Malaysia , 11800 – Mindern ,Pulau Pinang , Malaysia

[b] EMAN Research and Testing Laboratory, School of Pharmaceutical Sciences, Universiti Sains Malaysia , 11800 – Mindern ,Pulau Pinang , Malaysia

*Corresponding author: Dr. Teoh Siang Guan, PhD,
Professor
School of Chemical Sciences
Universiti Sains Malaysia
Penang-11800, Malaysia
E-mail: sgteoh@usm.my
H/P : (604) – 6577888

Fax : (604) - 6574854

**Graphical abstract**

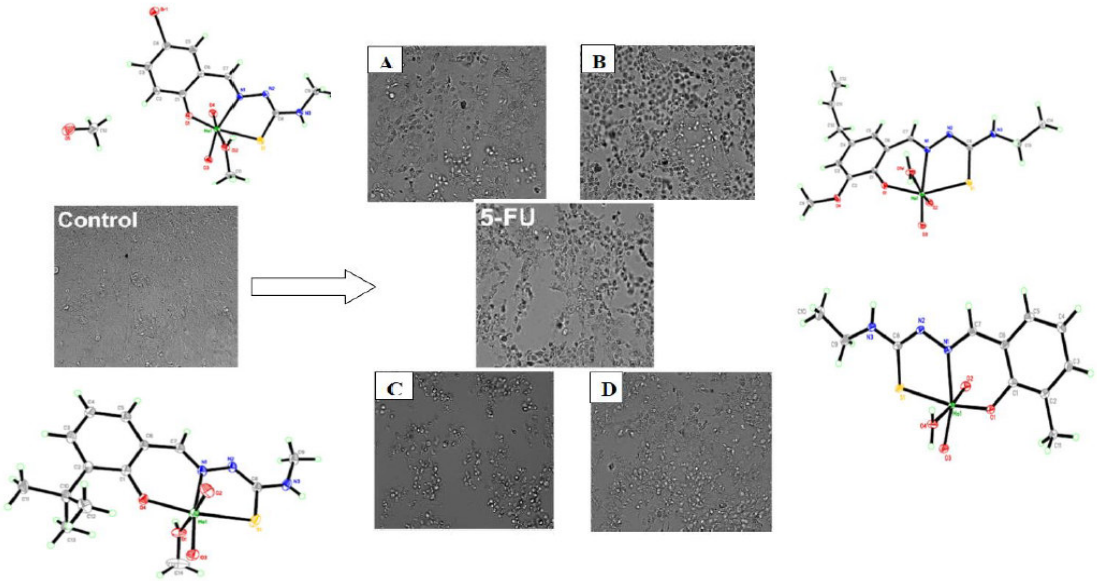


Photomicrographs of cell proliferation apoptosis by Mo (VI) complexes 1a-4a

# Mononuclear dioxomolybdenum(VI) thiosemicarbazonato complexes : Synthesis, structural characterization, *in vitro* DNA binding, cleavage, and antitumor properties

**Mouayed A. Hussein [a] , Teoh S. Guan [a *], Rosenani A. Haque [a] , Mohamed B. Khadeer Ahamed[b], Amin M.S. Abdul Majid[b]**

[a] School of Chemical Science , Universiti Sains Malaysia , 11800 – Mindern ,Pulau Pinang , Malaysia

[b] EMAN Research and Testing Laboratory, School of Pharmaceutical Sciences, Universiti Sains Malaysia , 11800 – Mindern ,Pulau Pinang , Malaysia

*Corresponding author: Dr. Teoh Siang Guan, PhD,
Professor
School of Chemical Sciences
Universiti Sains Malaysia
Penang-11800, Malaysia
E-mail: sgteoh@usm.my
H/P : (604) – 6577888

Fax : (604) - 6574854

**Highlights**

►Four Schiff bases derived from 4-ethyl (methyl) thiosemicarbazone were synthesized

►The ligands were coordinated with molybdenum(VI)

► The molecular structure of the complexes were characterized by x-ray single crystal

► DNA binding and DNA cleavage by the ligands and complexes were evaluated

► The activity of complexes against human colorectal (HCT 116) cell line was investigated